Planta
DOI 10.1007/s00425-016-2504-8

ORIGINAL ARTICLE

Overexpression of a synthetic insect–plant geranyl pyrophosphate synthase gene in *Camelina sativa* alters plant growth and terpene biosynthesis

Jing Xi[1] · Lorenzo Rossi[1] · Xiuli Lin[1] · De-Yu Xie[1]

Received: 10 February 2016 / Accepted: 17 March 2016

Abstract

Main conclusion **A novel plastidial homodimeric insect–plant geranyl pyrophosphate synthase gene is synthesized from three different cDNA origins. Its overexpression in *Camelina sativa* effectively alters plant development and terpenoid metabolism.**

Geranyl pyrophosphate synthase (GPPS) converts one isopentenyl pyrophosphate and dimethylallyl pyrophosphate to GPP. Here, we report a synthetic insect–plant *GPPS* gene and effects of its overexpression on plant growth and terpenoid metabolism of *Camelina sativa*. We synthesized a 1353-bp cDNA, namely *PTP-MpGPPS*. This synthetic cDNA was composed of a 1086-bp cDNA fragment encoding a small GPPS isomer of the aphid *Myzus persicae* (Mp), 240-bp *Arabidopsis thaliana* cDNA fragment encoding a plastidial transit peptide (PTP), and a 27-bp short cDNA fragment encoding a human influenza hemagglutinin tag peptide. Structural modeling showed that the deduced protein was a homodimeric prenyltransferase. Confocal microscopy analysis demonstrated that the PTP-MpGPPS fused with green florescent protein was localized in the plastids. The synthetic *PTP-MpGPPS* cDNA driven by 2 × 35S promoters was introduced into Camelina (*Camelina sativa*) by *Agrobacterium*-mediated transformation and its overexpression in transgenic plants were demonstrated by western blot. T_2 and T_3 progeny of transgenic plants developed larger leaves, grew more and longer internodes, and flowered earlier than wild-type plants. Metabolic analysis showed that the levels of beta-amyrin and campesterol were higher in tissues of transgenic plants than in those of wild-type plants. Fast isoprene sensor analysis demonstrated that transgenic Camelina plants emitted significantly less isoprene than wild-type plants. In addition, transcriptional analyses revealed that the expression levels of gibberellic acid and brassinosteroids-responsive genes were higher in transgenic plants than in wild-type plants. Taken together, these data demonstrated that this novel synthetic insect–plant *GPPS* cDNA was effective to improve growth traits and alter terpenoid metabolism of Camelina.

Keywords *Camelina sativa* · Isoprene · Geranyl pyrophosphate synthase · Prenyltransferase · Metabolic engineering · Synthetic biology · Terpene

Introduction

Terpenoids (isoprenoids) are biosynthesized from two common precursors, isopentenyl pyrophosphate (IPP) and dimethylallyl pyrophosphate (DMAPP) either from the mevalonate (MVA) pathway in the cytosol or from the 2-*C*-methyl-D-erythritol 4-phosphate (MEP) pathway in the plastids (Fig. 1). The first condensation step of IPP and DMAPP is catalyzed by geranyl pyrophosphate synthase (GPPS), which is a short chain prenyltransferase (also known as isopentyl pyrophosphate synthase), to produce a C_{10}-allylic geranyl pyrophosphate (GPP). Sequential addition of IPP to GPP leads to short chain (C_{15}–C_{25}), medium-chain (C_{30}–C_{35}), and long chain (C_{40}–C_n) prenyl pyrophosphate, which are then converted to a various

Electronic supplementary material The online version of this article (doi:10.1007/s00425-016-2504-8) contains supplementary material, which is available to authorized users.

✉ De-Yu Xie
dxie@ncsu.edu

[1] Department of Plant and Microbial Biology, North Carolina State University, Raleigh, NC 27695, USA

Published online: 29 March 2016

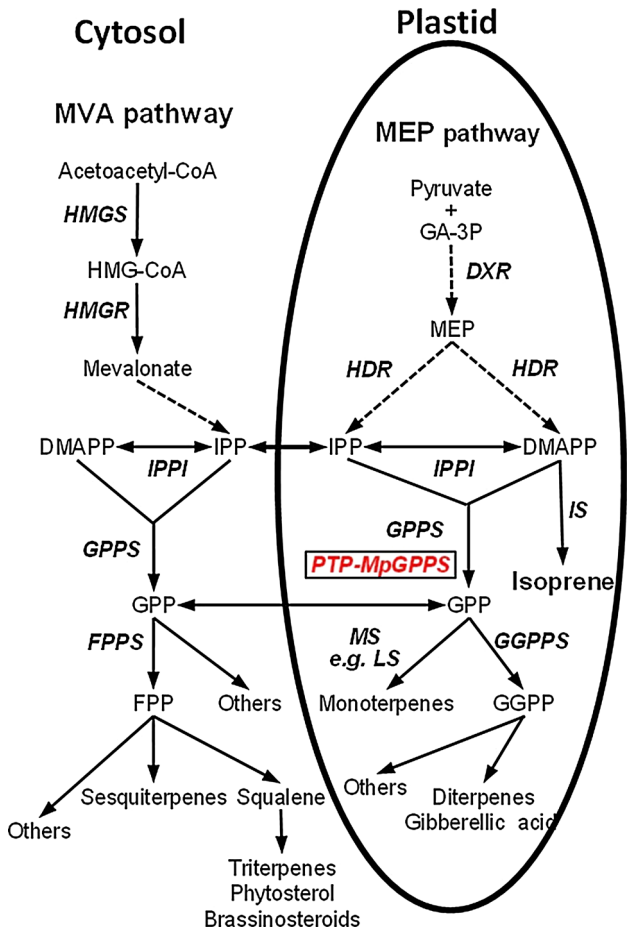

Fig. 1 Terpene biosynthesis starting with the MVA and MEP pathways. *Dashed arrows* indicate involvement of multiple enzymatic steps. The *solid two-end arrows* for IPP and GPP mean that these two intermediates are transported between plastids and the cytosol by unidentified transporters. The *box highlighted* indicates that our synthetic PTP-*MpGPPS* is overexpressed in transgenic *Camelina* plants. *HMGS* 3-hydroxy-3-methylglutaryl-CoA synthase, *HMG-CoA* 3-hydroxy-3-methyl-glutaryl CoA, *HMGR* 3-hydroxy-3-methylglutaryl CoA reductase, *GA-3P* D-glyceroldehyde-3-phophate, *DXR* 1-deoxy-D-xylulose 5-phosphate reductoisomerase, *MEP* 2-*C*-methyl-D-erythritol 4-phosphate, *HDR* 4-hydroxy-3-methylbut-2-enyl diphosphate reductase, *IPPI* isopentenyl diphosphate isomerase, *IPP* isopentenyl diphosphate, *DMAPP* dimethylallyl diphosphate, *IS* isoprene synthase, *GPPS* geranyl diphosphate synthase, *MpGPPS Myzus persicae* GPPS, *GPP* geranyl diphosphate, *MS* monoterpene synthase, *LS* limonene synthase, *FPPS* farnesyl diphosphate synthase, *FPP* farnesyl diphosphate, *GGPPS* geranylgeranyl diphosphate synthase, *GGPP* geranylgeranyl diphosphate

spectrum of C_{10}, C_{15}, C_{20}, and $C_{n>20}$-terpene products in the presence of terpene synthases (Fig. 1) (Tholl and Lee 2011; Wang and Ohnuma 2000). Isoprenoids play important roles in plant growth, plant pollination, and protection against herbivores (Lange 2015; Springob and Kutchan 2009). In addition, isoprenoids are main natural product sources for medicines (such as antimalarial artemisinin and anticancer paclitaxel), nutrients, perfumes, and other industrially important products (Lange 2015; Withers and Keasling 2007). Recently, short-chain isoprenoids gained interest as additives added to seed oil of *Camelina sativa* for biofuel (Borghi and Xie 2016; Tracy et al. 2009).

GPPS ([EC 2.5.1.1.]) is a short-chain isopentyl pyrophosphate synthase that is responsible for the enzymatic formation of GPP toward most monoterpenoids and diterpenoids in plastids (Nagegowda 2010; Schmidt et al. 2010; Vandermoten et al. 2009a) (Fig. 1). Although this enzyme was characterized in different organisms, *GPPS* genes were not cloned until the first cDNA was isolated from *Mentha* × *piperita* (peppermint) (Burke et al. 1999). To date, *GPPS* genes have been functionally characterized from approximately a dozen of plants (Gilg et al. 2005; Rai et al. 2013; Vandermoten et al. 2009b). Based on the quaternary structure, plant GPPS is classified into two types, heterodimeric (or heteromeric) and homodimeric (homomeric) (Chen et al. 2015; Hsiao et al. 2008; Nagegowda 2010; Rai et al. 2013; Schmidt et al. 2010). The active heterodimeric type is composed of a small subunit (SSU) and a large subunit (LSU). For example, the *Mentha* × *piperita* GPPS was characterized to be a heterodimer containing two subunits, one large (GPPS.LSU) and one small (GPPS.SSU). Two subunits show sequence similarity to a homodimeric geranylgeranyl pyrophosphate synthase (GGPPS, [EC 2.5.1.30.]) and contain a plastid-transit peptide sequence. The amino acid sequences of the GPPS.LSU share 56–75 % similarity to other reported GGPPSs. The GPPS.LSU contains a conserved aspartate-rich motif (D-D-x-x-x-x-D) that has been characterized to interact with pyrophosphate ester (Burke et al. 1999). However, the amino acid similarity between the GPPS.SSU and other reported GGPPSs is only 24–29 %, and the SSU lacks the conserved D-D-x-x-x-x-D motif (Burke et al. 1999). LSU and SSU alone are not catalytically active until their interaction forms an active heterodimeric complex that condenses IPP and DMAPP to GPP in peppermint (Burke et al. 1999). In addition, heterodimeric GPPSs were identified from other plants, such as hops (*Humulus lupulus*) (Wang and Dixon 2009) and *Catharanthus roseus* (Rai et al. 2013). In vitro analysis showed that GPPS.LSU alone from these two plants had catalytic activity to condense IPP and DMAPP to GPP and GGPP. When SSU and LSU form a heterodimeric complex, these two plants' GPPSs were found to alter the ratio of GPP and GGPP. Based on all investigations conducted, LSU is the catalytic subunit and SSU is the regulatory subunit. In particular, SSU is involved in regulating the chain length specificity (Burke and Croteau 2002b; Chang et al. 2010; Gutensohn et al. 2013b; Orlova et al. 2009). Homodimeric GPPSs were identified from two gymnosperm species (*Abies grandis* and *Picea abies*) (Burke and Croteau 2002a; Schmidt and Gershenzon 2008; Schmidt et al. 2010) and several

angiosperm species (such as *Arabidopsis thaliana*, *Lycopersicon esculentum*, *Quercus robur*, *Catharanthus roseus*, and *Phalaenopsis bellina*) (Rai et al. 2013). *In vitro* analyses have showed that recombinant homomeric GPPSs of *C. roseus* and *P. abies* only produce GPP, while recombinant GPPSs from other plants can produce GPP as a dominant and GGPP or FPP as a minor product. Additionally, genetic investigations have provided certain insights into *in planta* functions of homomeric GPPSs. In Arabidopsis and tomato, RNAi of *GPPS* leads to dwarfed phenotypes (van Schie et al. 2007b), indicating involvement in the biosynthesis of gibberellin (GA). To date, both homomeric and heteromeric GPPSs have been found to coexist in the same species, such as *C. roseus* (Rai et al. 2013) and *A. thaliana* (Chen et al. 2015; Hsieh et al. 2011). In *C. roseus*, the heteromeric GPPS but not the homomeric GPPS was found to be involved in the biosynthesis of monoterpene toward monoterpene indole alkaloids. These data indicate functional differentiation between heteromeric and homomeric GPPSs in one single plant species.

To date, *GPPS* genes have been identified in insects, e.g. *Myzus persicae* (Vandermoten et al. 2009b), *Ips pini* (Gilg et al. 2005), and *Phaedon cochleariae* (Frick et al. 2013). The aphid *M. persicae* produces monoterpene aggregation pheromones to coordinate colonization and mating. The *GPPS* cDNA cloned from *M. persicae* (namely *MpGPPS*) was characterized to encode a novel prenyltransferase that has a dual geranyl/farnesyl pyrophosphate synthase activity. This aphid was shown to express two GPPS isoforms, a long isoform (MpGPPS-L) and a short isoform (MpGPPS-S). The sequence of MpGPPS-L is only 32 amino acids longer than that of MpGPPS-S. The 32 amino acids are localized in the N-terminus of MpGPPS-L and contain an R-x-x-S motif, suggestive of mitochondrial targeting sequence (Martin et al. 2007). Other than these, the remaining amino acid sequences of the two isoforms are identical. Prenyltransferase activity analysis characterized that the catalytic efficiency of MpGPPS-S was approximately four times greater than that of MpGPPS-L, suggesting that the MpGPPS-S is the catalytically efficient form of the enzyme. The *GPPS* gene from *I. pini* (namely *IpGPPS*) was cloned from midgut and its expression is highly regulated by juvenile hormone III. In vitro analysis showed that IpGPPS mainly produces GPP (Gilg et al. 2005). In addition, the GPPS from *P. cochleariae* mainly produces GPP, but its activity is subject to regulation by metal ions.

Camelina sativa, also known as false flax or gold of pleasure, is an oilseed crop in the Brassicaceae family (Heller 1933; Kagale et al. 2014). It is an emerging biofuel crop for biodiesel and jet fuel products (Guy et al. 2014; Kagale et al. 2014; Kruczynski et al. 2012; Shonnard et al. 2010). Its seeds contain 36–47 % of oil that is composed of more than 90 % unsaturated fatty acids (Berhow et al. 2014). It is an appropriate oil crop to grow in marginal and acrid lands (Putnam et al. 1993; Shonnard et al. 2010). In addition, its growth in the field only needs low input of fertilizer (Putnam et al. 1993). These agronomic traits are superior over other oil crops for biofuel products, such as jet fuel, biodiesel, and high-value industrial lubricants (Moser 2012). In recent years, numerous investigations, such as field growth, oil composition modification, and omics, have been performed to develop Camelina as a potential resource for biofuel products (Choudhury et al. 2014; Ciubota-Rosie et al. 2013; Dalal et al. 2015; Kagale et al. 2014; Mudalkar et al. 2014; Nguyen et al. 2013, 2014; Park et al. 2014; Schillinger et al. 2012; Sun et al. 2014). In comparison, fewer studies have been conducted to engineer short chain terpenes in Camelina. Recently, a limonene synthase and a (+)-δ-cardinene synthase were introduced into Camelina seeds to achieve 0.7 % limonene and 0.5 % (+)-δ-cardinene (Augustin et al. 2015). Our group introduced a limonene synthase gene into Camelina and succeeded in increasing contents of limonene and 1,8-cinole in leaf, seed coat, and silique valve tissues using 35S, and seed coat and valve-specific promoters (Borghi and Xie 2016). Although continuous efforts are necessary, these promising successes have demonstrated that metabolic engineering provides opportunities to increase the production of monoterpenes and sesquiterpenes for Camelina biofuel products.

In this investigation, we aim to increase *in planta* catalytic efficiency of GPPS that controls the bottleneck step toward most of downstream isoprenoids and regulates plant performance. We selected the small isomer *GPPS* cDNA fragment of *M. persicae*, which encodes the highly efficient MpGPPS-S form as described above. Based on a previous investigation regarding overexpression of an animal farnesyl pyrophosphate synthase in tobacco plants (Wu et al. 2006), this type of small isomer *GPPS* cDNA fragment is unlikely subject to transcriptional or post-translational regulatory mechanisms operated in plants. Accordingly, we used the *MpGPPS-S* sequence as basis to synthesize a new cDNA, namely *PTP-MpGPPS*, which was composed of a fragment of Arabidopsis cDNA encoding a plastidial transit peptide, the small isomer *GPPS* cDNA fragment of *M. persicae*, and a cDNA fragment encoding a human influenza hemagglutinin tag. The *PTP-MpGPPS* was overexpressed in Camelina to generate multiple transgenic plants. Compared with wild-type plants, transgenic plants significantly reduced isoprene emission, but grew faster, developed larger leaf size and longer internodes, and flowered earlier. In addition, the levels of beta-amyrin and campesterol were increased in certain tissues of transgenic plants. The expression levels of genes that are specifically responsive to the increase of gibberellic acid and

brassinosteroids (BRs) were also increased in transgenic plants. These data demonstrated that a synthetic insect–plant *GPPS* gene is effective in regulating plant growth and terpene metabolism of Camelina.

Materials and methods

Plant materials and growth conditions

The Camelina variety used in all experiments was Calena. Seeds were surface-sterilized with 70 % (v/v) ethanol for 2 min, followed by 5 times of washing using autoclaved double deionized water. These seeds were further treated for 10 min using 50 % (v/v) bleach (3 % sodium hypochloride, KIK International Inc., ON, Canada) and then were washed five times using autoclaved double deionized water. Sterilized seeds were grown on a half-strength agar-solidified MS medium (Murashige and Skoog 1962). Seven-to ten-day-old seedlings were planted to Fafard 2P soil mix (Fafard, Inc., Anderson, SC) contained in white foam cups (8 Oz). Plants were placed in a growth chamber under a photoperiod of 16-h light/8-h darkness at 26 °C, and watered once a day. These growth conditions were also used to grow transgenic plants. Otherwise, any change is specified in the context.

Synthesis of a novel cDNA encoding a homodimeric insect–plant geranyl pyrophosphate synthase, development of constructs, and genetic transformation

The synthesis of a novel cDNA was conducted in three steps: selection of sequences, design, and synthesis. Sequences of cDNA fragments were selected from three different organisms. The first fragment was a partial cDNA sequence from *A. thaliana*. It consisted of the 1–240 bp nucleotides from the 5′-end of the full length coding DNA sequence (CDS) of *AtRBCS1A* (*at1g67090*) (Lee et al. 2008). This fragment was demonstrated to encode a plastidial transit peptide (PTP). The second fragment was a full length (1182 bp) of *GPPS* cDNA (AAY33491.1) from aphid *M. persicae (*Vandermoten et al. 2008). This cDNA was demonstrated to encode a monomeric protein with dual functions to catalyze the formation of both GPP and FPP. The third fragment was a 27-bp human influenza hemagglutinin (HA) tag cDNA sequence. After selection, the three cDNA fragments were designed together to obtain a novel cDNA encoding one protein targeted in plastids. The first 96 nucleotides (from 1 to 96) of the *MpGPPS* open reading frame (ORF) were replaced by the 240-bp *PTP* cDNA sequence. The 27-bp HA tag cDNA fragment was added at the end of the 3′-end of the *MpGPPS* ORF. The resulting novel cDNA was composed of 1353 bp nucleotides in length (S-Fig. 1). Finally, the 1353 nucleotides were synthesized by GenScript (GenScript USA Inc., Piscataway, NJ) and its sequence was submitted to gene bank.

The resulting novel *PTP-MpGPPS* cDNA was cloned to the immediate downstream of a 2 × 35S promoter of T-DNA in the binary vector pMDC84 (Curtis and Grossniklaus 2003). The resulting plant expression vector was named pMDC84-PTP-MpGPPS (Fig. 2c), in which GFP was fused at the end of PTP-MpGPPS. This new binary vector contained a hygromycin gene as selective marker. The T-DNA was then sequenced to confirm the accuracy of gene cloning. The binary plasmid was introduced into *Agrobacterium* strain GV3101. One positive colony of transformed GV3101 containing pMDC84-PTP-MpGPPS was used for floral dipping transformation by following a reported protocol (Lu and Kang 2008). GV3101-infiltrated plants (T_0) were continuously grown to produce T_0 seeds in the growth chamber to select transgenic progeny. The procedure is summarized in supplementary Figure 2. After seeds matured, they were harvested and then germinated on agar-solidified half-strength MS medium containing 15 μg/ml hygromycin (Fisher Scientific, Waltham, MA) to select resistant T_1 seedlings in the growth chamber (supplementary Figure 2). Similarly, T_2 and T_3 transgenic plants were screened to obtain homozygous progeny.

Modeling of PTP-MpGPPS

The synthetic cDNA was deduced to encode 451 amino acids. The amino acid sequence was uploaded to the publically available RaptorX website (Källberg et al. 2012; Peng and Xu 2011) for structural modeling. This software uses known proteins and their structures as template to model three-dimension structures of new proteins.

Transient expression assay of PTP-MpGPPS in *Nicotiana benthamiana*

In addition to the binary vector pMDC84-PTP-MpGPPS (Fig. 2c) described above, a positive binary vector was constructed as control. The fragment of 1–240 bp nucleotides (encoding a PTP) of *AtRBCS1A* (*at1g67090*) was cloned into pMDC84 using a Gateway Cloning System (Invitrogen, Carlsbad, CA). The resulting binary construct was named as 35S::RBCS1A:GFP (Fig. 2c) and then introduced to *Agrobacterium* strain GV3101 as positive control for transient expression assay. Two *Agrobacterium* GV3101 colonies, one containing pMDC84-PTP-MpGPPS and the other containing 35S::RBCS1A:GFP (Fig. 2c), were introduced into the epidermal cells of three-week-old *N. benthamiana* plants by infiltration as described previously (Sparkes et al. 2006), respectively. GFP fluorescence

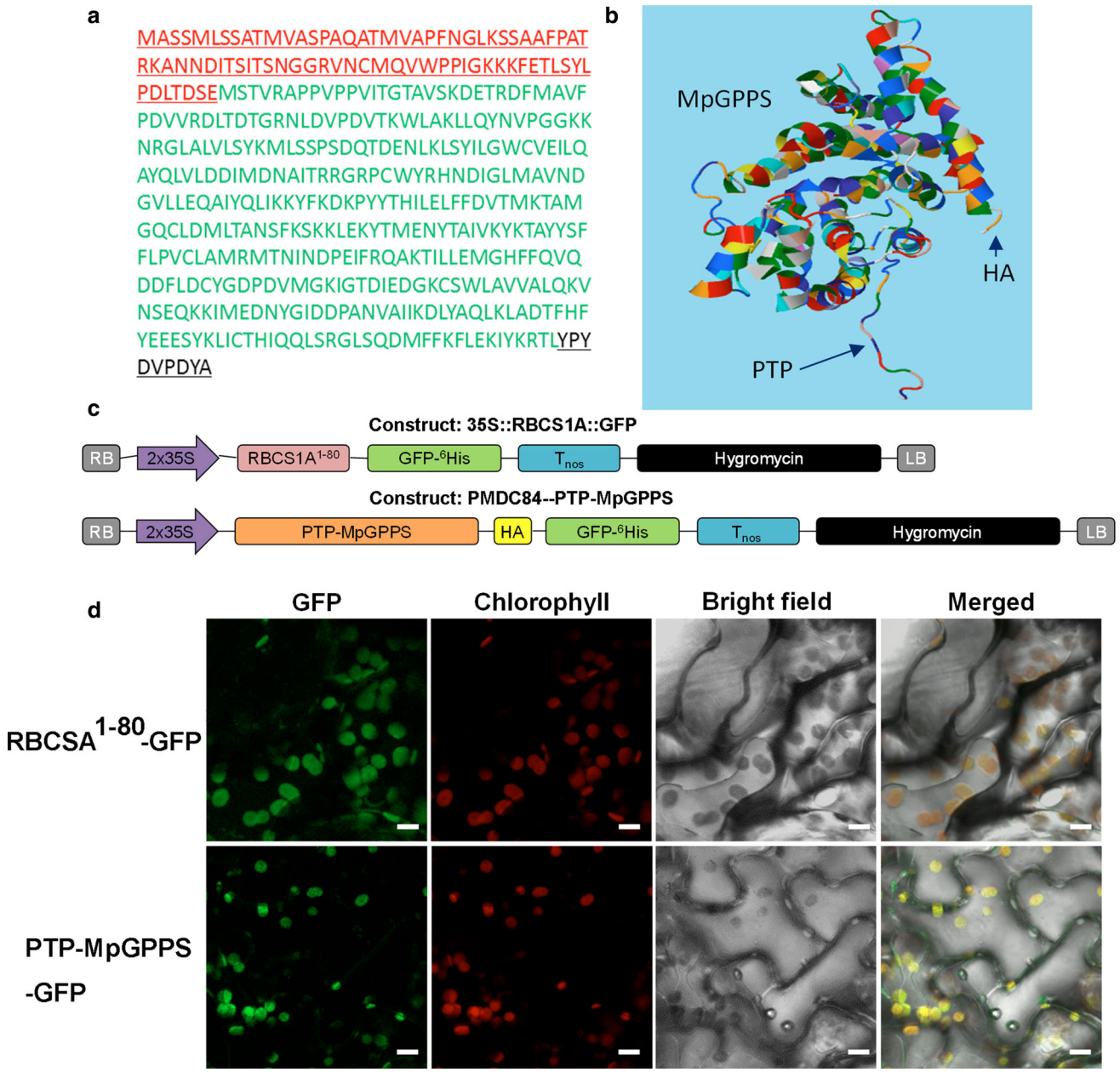

Fig. 2 Sequences, modeling, and constructs for genetic transformation and subcellular localization of PTP-MpGPPS. **a** 451 amino acids deduced from the synthetic cDNA, PTP: *red* capitalized amino acids, MpGPPS: *green* capitalized amino acids, and tag peptide: *black* capitalized amino acids. **b** Structure modeling shows PTP, MpGPPS and HA tag regions. **c** Schemes show two constructs developed from the pMDC84-GFP vector for genetic transformation and subcellular localization in the study; the *upper one* is the schematic of the 35S::RBCS1A:GFP vector as positive control. The *lower one* is the schematic of the pMDC84-PTP-MpGPPS vector to localize PTP-MpGPPS in plastids. The plasmids were developed using in-frame fusion of RBCS1A (1–80aa)/PTP-MpGPPS protein to the N terminus of GFP. *RB/LB* right/left border of pMDC84 vector, *2 × 35S* tandem cauliflower mosaic virus (CaMV) 35S promoter, *HA* human influenza hemagglutinin tag, *GFP^{6}His* green fluorescence protein with 6 histidine tag, *Tnos* nopaline synthase terminator. **d** Transient expression of plasmid DNAs containing RBCS1A (1-80aa)-GFP and PTP-MpGPPS-GFP in leaf mesophyll cells of *N. benthamiana*, respectively, the fluorescence of GFP (*green*), autofluorescence of chloroplast (*red*), and bright-field image (*gray*) were separately monitored using confocal microscopy and then all images were merged to localize the fused PTP-MpGPPS-GFP in mesophyll cells (*scale bar*: 20 μm)

was visualized and photographed using a Zeiss LSM 710 confocal microscope (Carl Zeiss AG, Jena, Germany). In addition, GFP alone is routinely used as negative control in our laboratory (Borghi and Xie 2016).

RNA isolation and real-time RT-PCR

Total RNA was isolated from 4-week-old plants using the RNeasy Plant Mini Kit (Qiagen, Hilden, Germany), and

then treated with DNase I (RNase free DNase set; Qiagen) to clean up the potential contamination of genomic DNA. The concentration of total RNA was quantified using a NanoDrop 2000C spectrophotometer (NanoDrop products, Wilmington, DE). The first-strand cDNAs were synthesized using SuperScript® First-Strand Synthesis System for RT-PCR (Invitrogen, Carlsbad, CA). Subsequent real-time RT-PCRs were performed with Power SYBR® Green PCR Master Mix (Applied Biosystems, Warrington, UK) to analyze gene expression on a StepOnePlus™ Real-Time PCR Instrument (Applied Biosystems, Warrington, UK), and fluorescence was analyzed using StepOne™ software v2.2.2. The relative expression levels of target genes were calculated by normalizing their expression levels against the housekeeping gene *Tubulin18*.

Western blot analysis

Thirty mg leaf samples from 4-week-old plants were ground into fine powder in liquid N_2. The powder was suspended in 100 µl of protein extraction buffer, which was composed of 50 mM Tris–HCl, pH 8.0, 5 mM EDTA, and 0.2 % β-mercaptoethanol (v/v). In addition, the extraction buffer was supplemented with the Complete Protease Inhibitor Cocktail Tablet (Roche Applied Science, Penzberg, Germany). Protein content was determined by the Bradford reagent (Bio-Rad, Hercules, CA). Equal amount of total protein (20 µg) from each sample was subjected to SDS-PAGE and subsequently transferred to polyvinylidene fluoride (PVDF) membrane (Millipore, Billerica, MA). After blocking with 2 % non-fat milk in TBST buffer (50 mM Tris–HCl, pH 7.5, 150 mM NaCl, 0.05 % Tween-20), the membrane was incubated in the same buffer containing 1/5000 dilution of 1st Ab–goat anti HA-tag (GenScript). After three times of washing with TBST buffer, the membrane was incubated with 2 % non-fat milk in TBST buffer containing 1/10,000 dilution of 2nd Ab–donkey anti-goat IgG-HRP (Santa Cruz Biotechnology, Dallas, TX). The signal was detected with the SuperSignal West Pico Chemiluminescent Substrate (Fisher Scientific, Waltham, MA).

Measurement of plant height, leaf size, internode number, and internode length

The plant height was measured from the soil surface to the arch of the uppermost leaf using a ruler. Leaf arrangement of Camelina is featured by an alternative phyllotaxy. Each leaf has a short petiole. The length of each leaf was measured from the tip to the base of the short petiole. The resulting numbers were used to represent leaf sizes. The internode number was defined by the number of leaves on the main stem (Carvalho et al. 2002). The internode length was obtained by measuring the distance between two successive main stem leaves. All measurements were conducted for plants that were planted at the same time and grown in the same condition.

Gas chromatograph-mass spectrometer analysis

Flowers and stems were collected from transgenic vs. wild-type plants and immediately frozen in liquid nitrogen. Samples were ground into fine powder in liquid nitrogen. Two hundred milligram of powder was measured into a 1.5-ml tube. Each tube was added 50 ng/µl 5α-cholestan-3β (Sigma-Aldrich, St. Louis, MO) as internal standard. Each tube was added 2 ml dichloromethane (Sigma-Aldrich, St. Louis, MO) and completely mixed by vortexing 1 min and then 10 min sonication at room temperature. Tubes were centrifuged at 12,000 rpm for 10 min to obtain the upper supernatant and the bottom pellet phases. The supernatant extraction was pipetted to a new 1.5 ml tube. This step was repeated once to obtain total 400 µl extraction. One µl extraction was injected to Agilent 5890 gas chromatography coupled with 5972 series II mass spectrometry (Agilent, Santa Clara, CA) as previously described (Almaarri et al. 2010). Peak areas of metabolites were recorded on MSD ChemStation G1701EA E.02.02.1431. Authentic β-amyrin and campesterol were purchased from Sigma and standard curves were developed for both of them. Contents of metabolites were calculated using the standard curves.

Measurement of isoprene emission by fast isoprene sensor

Plants were grown in the greenhouse (temperature: 20–26 °C; relative humidity: 55–75 % day-night; 10/14 h photoperiod (light/dark); and 400 µmol m^{-2} s^{-1} maximum light intensity). Plants were supplied with 1 g/l of Osmocote (The Scotts Miracle-Gro Company, Marysville, OH) bi-weekly for 20 days. After 30 days of seed germination, three plants of each genotype were grouped as one biological sample and then placed in a sealed transparent plastic round-shape chamber (40 cm in diameter) connected with the Fast Isoprene Sensor (FIS, Hills Scientific, Inc., Boulder, CO, USA; Guenther and Hills 1998). Then, an oxygen cylinder (sufficient for 48 h) was connected to FIS. After FIS was calibrated with the isoprene standard, non-stop measurement was conducted for 48 h to record isoprene emission. At the end of the experiment, all plants were carefully weighed to obtain fresh weights. The order of measurement was wild-type plants and then transgenic plants. Three biological samples for each genotype were measured; therefore, it took 1 week period to measure one genotype. Isoprene was converted to photons by FIS. Photons emitted every 5 s were recorded by computer

using the specific FIS software. During the measurement period, light intensity was examined daily at noon to ensure consistency during each measurement. The light intensity was in the range of 300–400 μmol m^{-2} s^{-1}, which was similar for both transgenic and wild-type plants during the measurement. Based on the following equation formula, the emission rate was calculated to compare both wild-type and transgenic plants.

In addition, leaves were detached from plants grown in growth chamber to measure isoprene emission at room temperature and room light condition. The measurement time was 1 h. The measurement procedures were the same as described above.

Data were exported from the FIS software to Microsoft Excel sheet and then elaborated. The concentration of isoprene measured by the FIS was volumetric, ppbv (part per billion in volume). The initial isoprene concentration measured before starting the experiment was 160 ppbv in the chamber. Final data were calculated based on the following instrumental parameters: (1) leak rate into chamber is 1.1 slpm (standards liters per minute), matching extraction flow rate into FIS; (2) the 160 ppbv isoprene level can be maintained continuously; (3) the leak air entering in the chamber contains 0 ppbv isoprene.

Based on the above mentioned parameters, flux of isoprene from plants was calculated by:

$$\text{Concentration} \times \text{flow}$$

$$\text{Flux} = \left(\frac{160\times10^{-9}\text{L isoprene}}{1\text{ L air}}\right)\left(\frac{1\text{ mol isoprene}}{22.4\text{ L isoprene}}\right) \times \left(\frac{1.1\text{ L air}}{1\text{ min}}\right)\left(\frac{60\text{ min}}{1\text{ h}}\right)\left(\frac{24\text{ h}}{1\text{ day}}\right)$$

$$\text{Flux} = \left(\frac{1.13\times10^{-5}\text{ mol isoprene}}{1\text{ day}}\right)$$

$$\text{Flux} = \left(\frac{1.13\times10^{-5}\text{ mol isoprene}}{1\text{ day}}\right)\left(\frac{68.1\text{ g isoprene}}{1\text{ L isoprene}}\right)$$

$$\text{Flux} = \left(\frac{7.7\times10^{-4}\text{ g isoprene}}{1\text{ day}}\right) \quad (1)$$

Therefore, the isoprene flux rate per gram of fresh plant material is calculated based on Eq. (2)

$$\text{Flux/g FW} = \left(\frac{1.13\times10^{-5}\text{ mol isoprene}}{1\text{ day}}\right) \times \left(\frac{1}{\text{g fresh plant material}}\right) \quad (2)$$

Statistical analysis

Student *t* test was carried out to evaluate significant differences in values of qRT-PCR, metabolite estimation, and plant growth measurement. Error bars represent standard deviation.

Results

Synthesis of an insect–plant geranyl pyrophosphate synthase cDNA

A 1353-bp cDNA was synthesized from three different cDNA origins. The first one is a 240-bp cDNA fragment from Arabidopsis and encodes a plastidial transit peptide (PTP) consisting of 80 amino acids. The second one is a 1086-bp cDNA fragment from the aphid *M. persicae* and encodes a truncated GPPS consisting of 362 amino acids. The third one is a 27-bp cDNA fragment that encodes a short human influenza hemagglutinin tab (HA tag) peptide (S-Fig. 1). The resulting synthetic cDNA was named as *PTP-MpGPPS* in this study and its gene bank accession number is KU645998. It was deduced to encode 451 amino acids that are composed of three synthetic regions (Fig. 2a). An online structure modeling was carried out using RaptorX (Källberg et al. 2012; Peng and Xu 2011). The best template (*P* value: 1.86E−08) resulting from modeling was a homodimeric avian farnesyl pyrophosphate synthase (Tarshis et al. 1996). The resulting model showed that the PTP-MpGPPS protein included three synthetic regions, PTP (the helix at the $–NH_2$ end), MpGPPS (ribbons and helixes), and HA (the helix at the –COOH end) (Fig. 2b). This modeling also showed that there was no interaction among these three regions.

Localization of PTP-MpGPPS in plastids

To demonstrate whether or not the synthetic *PTP-MpGPPS* could encode a protein localized in plastids, it was fused to the 5-end of a green fluorescence protein (GFP) contained in the binary construct pMDC84 (Invitrogen, Carlsbad, CA) (Fig. 2c). The resulting recombinant construct pMDC84-PTP-MpGPPS was introduced into leaf cells of *N. benthamiana* by an infiltration of *Agrobacterium*-mediated transformation. In addition, a positive control construct for plastidial localization of GFP, namely 35S::RBCS1A:GFP, was introduced into leaf cells of *N. benthamiana.* Cellular images of green fluorescence of GFP, red fluorescence of chlorophyll, and bright cells were photographed under a confocal microscope. The resulting merged image showed that the fused PTP-MpGPPS-GFP was localized in the plastids (Fig. 2d). Confocal microscopic images also showed that the positive control was localized in the plastids (Fig. 2d). Localization of GFP alone as a negative control is routinely performed in different plant species such as Camelina and *N. benthamiana*

in our laboratory. For example, our recent report showed that GFP alone was localized in the cytosol (Borghi and Xie 2016). These results demonstrated that the synthetic *PTP-MpGPPS* cDNA encoded a protein that was transported into the plastids.

Ectopic expression of *PTP-MpGPPS* promotes plant growth and early flowering

The *PTP-MpGPPS* transgene driven by 2 × 35S promoter in the binary vector pMDC84-PTP-MpGPPS (Fig. 2c) was successfully transformed into Camelina by following an *Agrobacterium*-mediated transformation protocol (Lu and Kang 2008). Hygromycin-resistant T_1 transgenic lines were selected on a selection medium (S-Fig. 3a). PCR amplified both *hygromycin* and *GFP* in the T-DNA (S-Fig. 3b) from the genomic DNA of putative T_1 transgenic lines, indicating successful transformation. Furthermore, western blot analysis using HA antibody demonstrated that 5 T_1 lines (namely T_1-#7, #10, #11, #16, #17) translated the synthetic gene to a protein (Fig. 3a, S-Fig. 3c). By contrast, the western blot results were negative for non-transgenic T_1 azygous lines (e.g. #6, #8, #9 and#12) (Fig. 3a), wild-type, and vector control transgenic plants (Fig. 3a, S-Fig. 3c).

The ectopic expression of *PTP-MpGPPS* altered plant growth and development of progeny of transgenic plants. The average values for plant height, leaf size, internode number and length, and growth days reaching to flowering time were recorded in details at different time points during the growth period of transgenic progeny. From seed germination to the time immediately prior to flowering, T_2 progeny of T_1-#11 (Fig. 3b and c), #7 (S-Fig. 4a), and #10 (S-Fig. 4b) grew faster than wild-type plants. The height of these T_2 progeny that were measured at different growth stages was higher than that of wild-type plants (Fig. 3d–f). However, the height of vector control transgenic and wild-type plants was similar (S-Fig. 5). In addition to comparing plant growth, RT-PCR was completed to further confirm the overexpression of the synthetic *PTP-MpGPPS* transgene in T_2 progeny (S-Fig. 6). Seeds of T_2 plants were further screened on the selection medium to obtain a large number of hygromycin-resistant T_3 progeny seedlings. T_3 progeny plants from each of T_1-#7, #10 and #11 lines grew faster than wild-type plants (Fig. 3g–i), demonstrating that these progeny inherited the faster growth trait resulted from the synthetic transgene.

From the bottom to the upper nodes, the average leaf sizes of T_3 transgenic progeny were significantly larger than those of wild-type plants at the same position (Fig. 4a, b). Prior to flowering, the numbers of nodes of T_3 transgenic progeny were more than those of wild-type ones. The lengths of internodes of T_3 transgenic progeny were longer than those of wild-type ones at the same position (Fig. 4d, e).

Fig. 3 Effects of the PTP-MpGPPS overexpression on plant growth. ▶ **a** A western blot image shows the expression of PTP-MpGPPS in different T_1 lines (#7, #10, and #11) of transgenic plants. **b** An image shows growth phenotypes of 4-week-old T_2 progeny of line #11 vs. wild-type (WT) plants grown under the photoperiod of 16/8 h (light/dark) at 25 °C. **c** An image shows growth phenotypes of 6-week-old T_2 progeny of line #11 vs. WT plants grown under the photoperiod of 16/8 h (light/dark) at 25 °C. Plant heights show elongation difference between T_2 progeny of line #11 and WT plants (4- and 6-week-old) (**d**), between T_2 progeny of line #7 and wild-type plants (5-week-old) (**e**), between T_2 progeny of line #10 and wild-type plants (5-week-old) (**f**). Plant heights show elongation difference of T_3 progeny of line #7 and wild-type plants (5- and 6-week-old) (**g**), T_3 progeny of line #10 and wild-type plants (4- and 5-week-old) (**h**), and T_3 progeny of line #11 and wild-type plants (4-, 5- and 6-week-old) (**i**). Data represent average and standard deviation values of at least nine measurements ($n \geq 9$). $^{**}P < 0.01$, $^{*}P < 0.05$, Student's *t* test

The flowering time of T_3 transgenic progeny was 2–3 days earlier than those of wild-type ones. All of these phenotypes were also observed in the T_2 homozygous progeny. However, all of these altered phenotypes were not observed in vector control transgenic plants.

Reduction of isoprene emission from transgenic plants

It has been unknown whether wild-type Camelina can produce isoprene via DMAPP in plastids (Fig. 1). Fast isoprene sensor (FIS) has been developed to specifically measure isoprene emission (Exton et al. 2010). The mechanism is that isoprene is converted into photon in the presence of ozone that is generated from oxygen provided by oxygen cylinder. Isoprene-derived photon signals are counted by a special photons counter inside the instrument. FIS detected isoprene emission from wild-type Camelina plants grown in both laboratory (also growth chamber) (Fig. 5a) and greenhouse (Fig. 5b) conditions during the winter time of 2014 and 2015. Isoprene emission was recorded every 5 s to characterize profiles. The resulting data showed that isoprene emission profiles were dynamic during a diurnal cycle (Fig. 5b). Plants placed in a chamber were continuously measured 48 h to estimate emission rate per day. After calculation of 1 week measurement, an emission rate was estimated to be approximately 0.2 mg/day, per g FW in greenhouse during the winter time (Fig. 5c).

FIS was also used to measure daily isoprene emission from T_3 transgenic progeny grown in the same conditions used for wild-type plants. Results from recordings of emission dynamics consistently showed the reduction of isoprene emission from transgenic plants in both greenhouse and growth chamber conditions compared to wild-type plants (Fig. 5a, b). Quantification was performed to calculate isoprene emission from transgenic plants in 1 week period. The resulting data showed that the emission

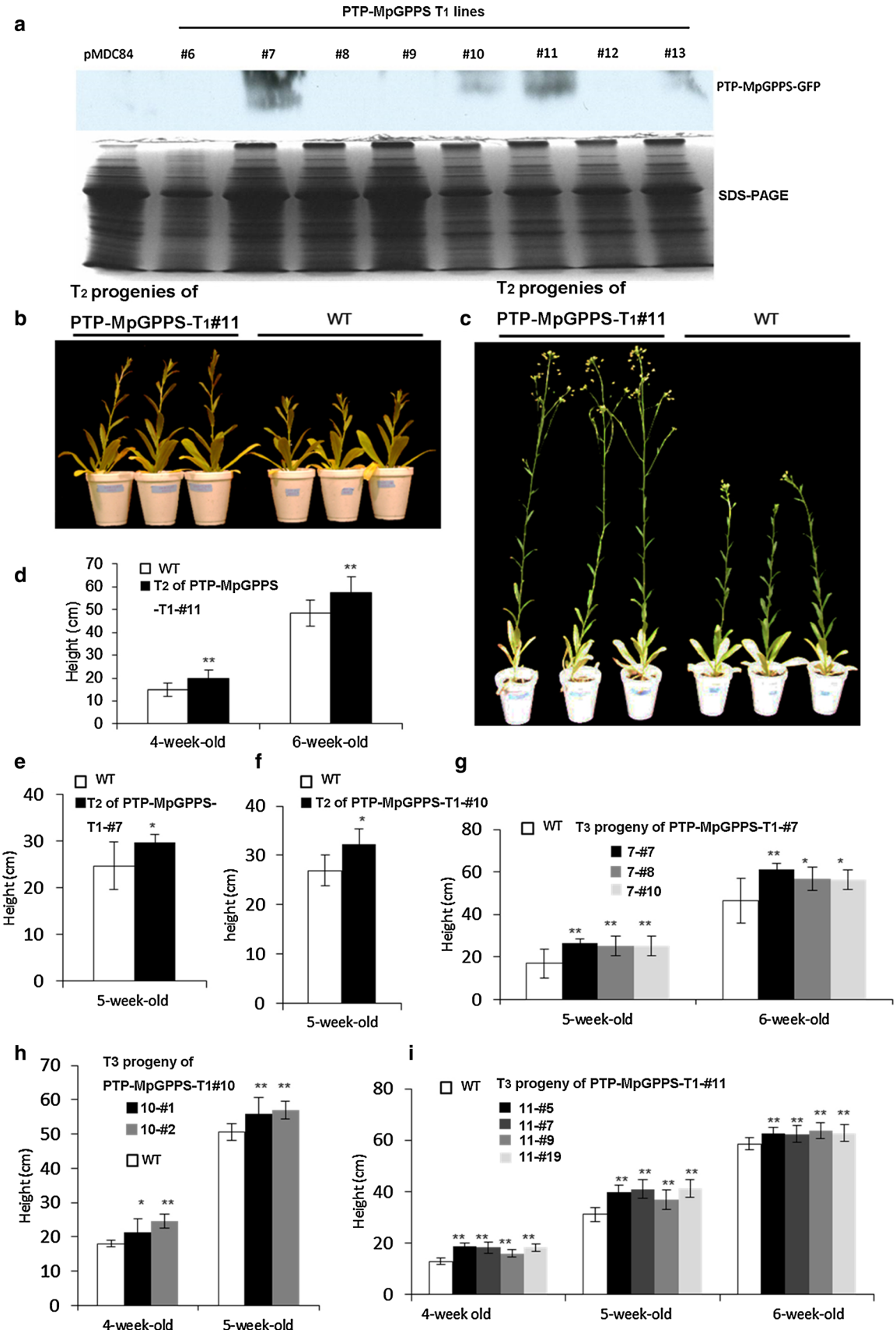
a
PTP-MpGPPS T1 lines
pMDC84
#6
#7
#8
#9
#10
#11
#12
#13
PTP-MpGPPS-GFP
SDS-PAGE
b
T2 progenies of
PTP-MpGPPS-T1#11
WT
c
T2 progenies of
PTP-MpGPPS-T1#11
WT
d
WT
T2 of PTP-MpGPPS
-T1-#11
Height (cm)
4-week-old
6-week-old
e
WT
T2 of PTP-MpGPPS-
T1-#7
Height (cm)
5-week-old
f
WT
T2 of PTP-MpGPPS-T1-#10
height (cm)
5-week-old
g
WT
T3 progeny of PTP-MpGPPS-T1-#7
7-#7
7-#8
7-#10
Height (cm)
5-week-old
6-week-old
h
T3 progeny of
PTP-MpGPPS-T1#10
10-#1
10-#2
WT
Height (cm)
4-week-old
5-week-old
i
WT
T3 progeny of PTP-MpGPPS-T1-#11
11-#5
11-#7
11-#9
11-#19
Height (cm)
4-week old
5-week-old
6-week-old

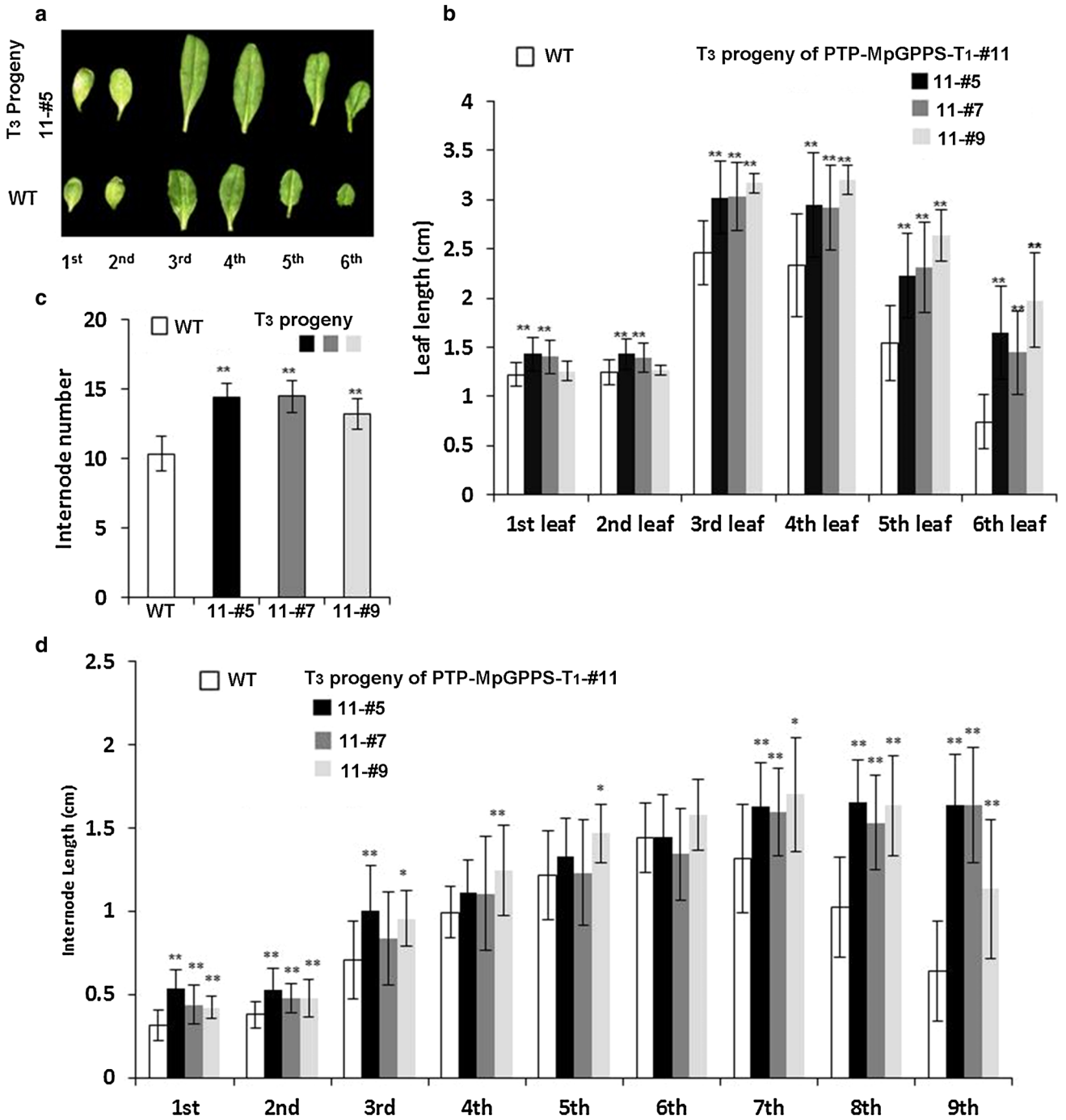

Fig. 4 Effects of the PTP-MpGPPS overexpression on plant development. **a** An image shows leaf morphology of the first six nodes on stems of 2-week-old T_3 (#5) progeny of line #11 vs. WT plants. **b** Data show the length of the first six leaves of 2-week-old T_3 progeny (#5, #7 and #9: three independent T_3 progeny from line T_1#11) vs. WT plants. **c** Data show the internode number of 4-week-old T_3 progeny vs. WT plants. Internodes were numerated from the *bottom* to the *top*. **d** Data show the length of the first nine internodes measured from 4-week-old T_3 progeny vs. WT plants. Data represent average and standard deviation values of at least nine measurements ($n \geq 9$). $^{**}P < 0.01$, $^{*}P < 0.05$, Student's *t* test

rate of isoprene was approximately 0.14 mg/day per g FW in transgenic plants, significantly lower than in wild-type plants (Fig. 5c). These results indicated that the ectopic expression of the synthetic *PTP-MpGPPS* in plastids competitively converted DMAPP to downstream terpenes.

Increase of β-amyrin and campesterol in transgenic plants

Gas-chromatography coupled with mass spectrometer analysis was employed to analyze other terpenes in T_3

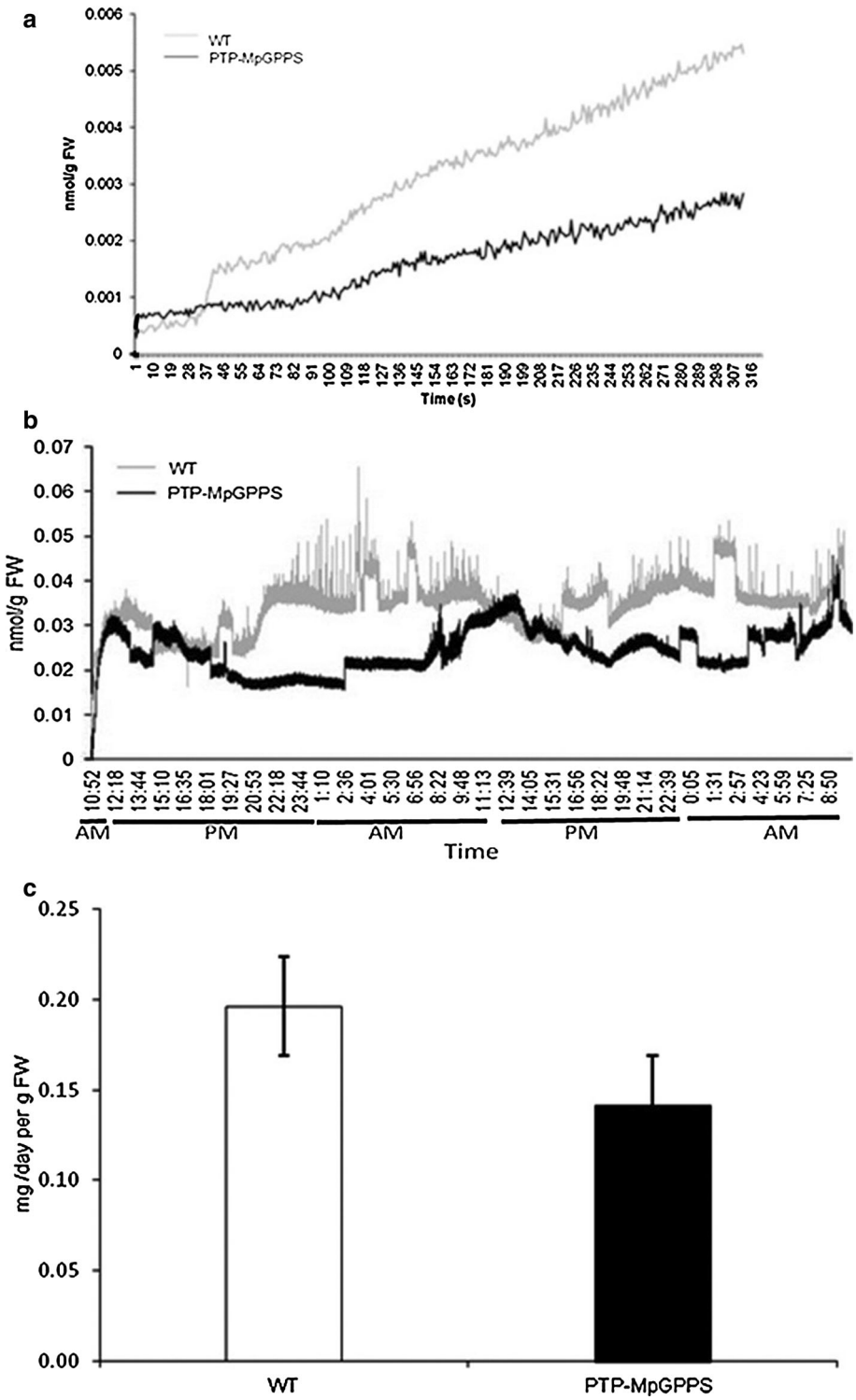

Fig. 5 Isoprene emission from Camelina and effects of the *PTP-MpGPPS* overexpression on isoprene emission from transgenic plants. **a** Isoprene emission from Camelina leaves was recorded for approximately 5 min using a fast isoprene sensor in the laboratory under a low illuminant lighting condition; **b** Isoprene emission from *PTP-MpGPPS* T_3 progeny transgenic vs. and WT plants were continuously recorded 48 h using a fast isoprene sensor in green house; **c** comparison of daily isoprene emission from the *PTP-MpGPPS* T_3 transgenic vs. WT plants. Data were exported from the FIS software to Excel sheet and elaborated. Flux of isoprene from plants was calculated by this formula (2)

transgenic vs. wild-type control plants. Campesterol and β-amyrin (Fig. 6a) were identified using standard samples and searching the NIST library. Quantification using a standard curve showed that the contents of β-amyrin were significantly higher in flowers and stems of transgenic plants than those of wild-type ones (Fig. 6b). The content of campesterol was significantly higher in stems of transgenic plants than those of wild-type ones (Fig. 6b). In addition, additional peaks were detected in samples. Although the nature of these metabolites was unknown,

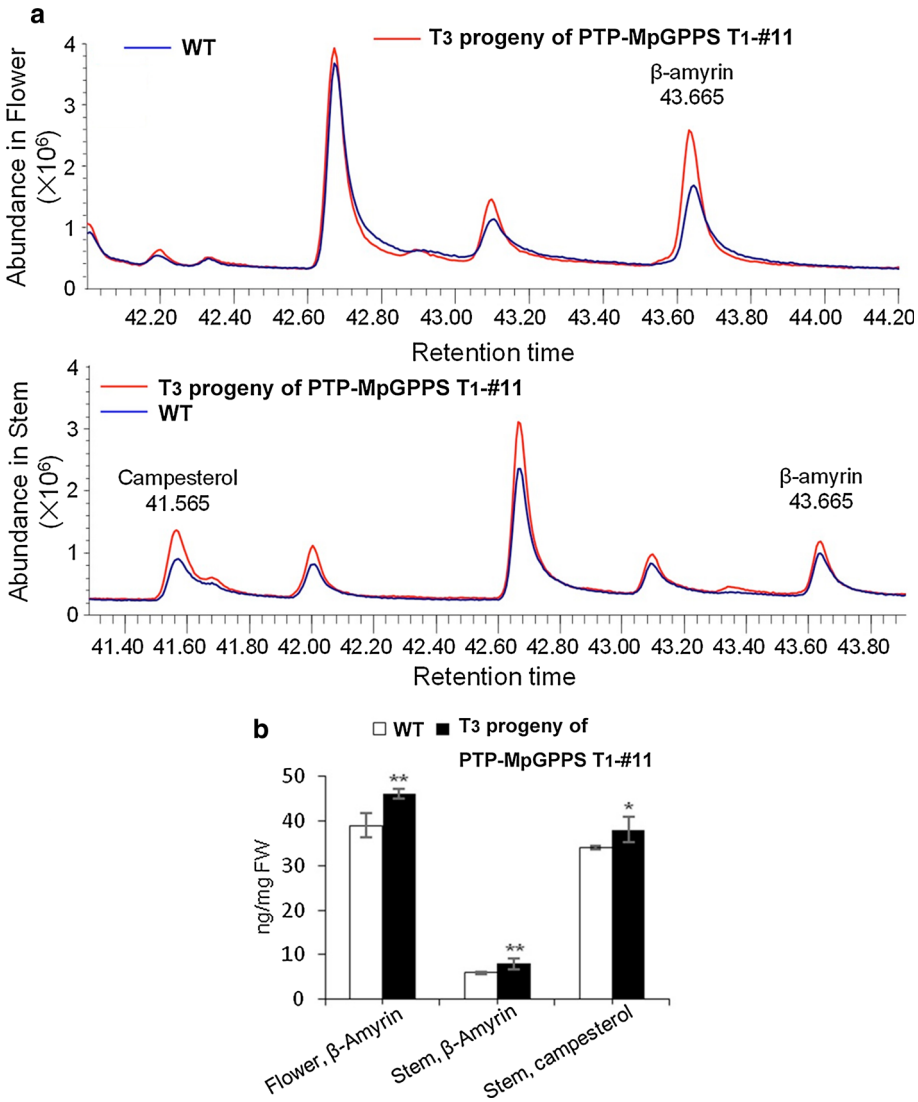

Fig. 6 Effects of the *PTP-MpGPPS* overexpression on production of triterpene and phytosterol in transgenic vs. WT plants. **a** Total-ion chromatography of GC–MS showing β-amyrin and campesterol detected in flower and stem samples of 4-week-old *PTP-MpGPPS* T_3 progeny transgenic and WT plants; **b** contents of β-amyrin and campesterol in flower and stem tissues of 4-week-old *PTP-MpGPPS* T_3 progeny transgenic vs. WT plants

their peak area values were higher in transgenic plants than in wild-type ones (Fig. 6b). These compounds remain to be identified in the future.

Up-regulation of genes responsive to gibberellin and brassinosteroid in transgenic plants

The analysis of qRT-PCR was carried out to understand whether genes responsive to GA and BR signals were up-regulated in transgenic plants. *EXP8* and *SCL3* that are two representative GA-responsive marker genes have been used to estimate alterations of GA levels in plants (Park et al. 2013). The transcriptional levels of the two genes were examined in 4-week-old plants. The results of qRT-PCR showed that the expression levels of these two genes were increased 1.2 fold (P values <0.01) in transgenic plants compared to wild-type ones (Fig. 7). Based on the regulation of plant growth and development by GA, this result suggested a potential increase of GA level in transgenic plants. *AGP4*, *EXP5*, and *δ-TIP* are three BR-responsive marker genes (Coll-Garcia et al. 2004). The results of qRT-PCR showed that the expression levels of these three genes were significantly increased in transgenic plants compared to wild-type (Fig. 7), suggesting a potential increase of BR levels.

Discussion

Our investigation showed that a novel synthetic plant–insect *GPPS* coupled with a genetic transformation approach could effectively alter plant growth and terpenoid metabolism. The *PTP-MpGPPS* cDNA was synthesized from three cDNA fragments, an Arabidopsis *PTP* cDNA, an aphid *GPPS* cDNA, and a HA tag cDNA fragment. After the synthetic cDNA was integrated into the genome of

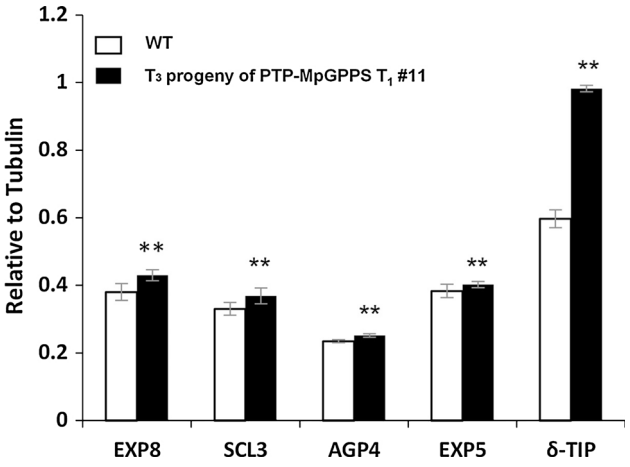

Fig. 7 Effects of the *PTP-MpGPPS* overexpression on transcriptional levels of GA-responsive genes and BR-responsive genes in transgenic plants. Real-time RT-PCR analysis was carried out to compare the expression levels of two GA-responsive genes that were *EXP8* and *SCL3*, and three BR-responsive genes that were *AGP4*, *EXP5*, and *δ-TIP*, in 4-week-old *PTP-MpGPPS* T_3 transgenic vs. WT plants. The Camelina Tubulin18 gene was used as the internal control. Data represent average and standard deviation values of at least three measurements. $^{**}P < 0.01$, Student's *t* test

Camelina, its overexpression led transgenic plants to grow faster, elongate longer internodes, develop more nodes, increase leaf sizes, and promote early flowering (Figs. 3, 4, S-Fig. 4). In addition, the overexpression of the synthetic *PTP-GPPS* led to significant reduction of isoprene production (Fig. 5b, c). By contrast, its overexpression increased levels of downstream triterpenes and steroids in tissues (Fig. 6). These data demonstrate that a small insect GPPS unit is catalytically functional in plants and a synthetic approach is of agricultural significance for improvement of agronomic traits. In addition, these data show a potential application significance of the synthetic cDNA in "capturing isoprene". Six hundred million tons of isoprene is estimated to be annually released to the atmosphere by plants (Guenther et al. 2006). In addition, given that the emission of isoprene is highly enhanced by high temperature (e.g. 30–35 °C) and lighting condition (Arneth et al. 2008; Schnitzler et al. 1997; Sharkey et al. 1996, 1999; Singsaas and Sharkey 2000), it can be predicted that the global climate change likely increases isoprene emission. Isoprene emission is not only a loss of photo-assimilated carbon (photosynthesis), but also a significant source of air-pollution and global climate change. It has been reported that high levels of isoprene are emitted by agro-forest species or other plants to cause local or regional ozone pollution (Andersson and Engardt 2010; Arneth et al. 2011; Lee et al. 2006; Rosenstiel et al. 2003). The increase of isoprene can also cause enhancement of methane lifetime (Arneth et al. 2011), a factor associated with global climate change. These pollutions necessitate development of new technology to convert the massive production of isoprene to biomass and energy. In our experiments, we measured isoprene during winter time. The rationale is that most previous investigations reported isoprene emission only from certain numbers of trees in summer time and tropical plants but not from every plant species, particularly herbaceous species in non-tropical regions (Monson et al. 2013; Sharkey 2013). Our measurement provided evidence that herbaceous plants such as Camelina can emit isoprene even during winter time. Our results also demonstrated that a synthetic PTP-MpGPPS could reduce isoprene to lead to production of other terpenoids during short photoperiod and low temperature season. Therefore, our experiments not only provide proof of concept in reduction of isoprene emission, but also these data show that a synthetic biology approach has potential to capture this simple hydrocarbon molecule.

The improvement of vegetative growth and early flowering of *PTP-MpGPPS* transgenic plants likely resulted from the increase of GAs and BRs *in planta*. As well characterized, bioactive GAs (e.g. GA3) regulates plant growth and development such as stem elongation, leaf expansion, flower and fruit development (Olszewski et al. 2002; Yang et al. 1996) and BR also promotes stem elongation (Grove et al. 1979). Due to difficulties in analysis of in vivo GA and BR levels, GA- and BR-responsive genes have been used as appropriate biomarkers to understand if the levels of the two hormones are likely increased in plants (Coll-Garcia et al. 2004; Park et al. 2013). In our experiments, qRT-PCR analysis showed that the transcriptional levels of two GA-responsive genes (*EXP8* and *SCL3*) and three BR-responsive genes (*AGP4*, *EXP5* and *δ-TIP*) (Coll-Garcia et al. 2004) were significantly increased in transgenic plants. In addition, the association between the alteration of Camelina plant growth and GA increase can be supported by evidence of other plant GPPS researches. GPPS's activities and GPP's contents have been genetically demonstrated to associate with plant development, functions, and metabolisms. A reduction of *GPPS* expression level in tomato (*Lycopersicon esculentum*) was reported to cause plant dwarf, this phenotype of which was considered to associate with a reduction of GA derived from GPP. When the dwarf tomato plants were treated with exogenous GA, the growth was rescued to normal height. The silencing of *AtGPPS* also resulted in a dwarf phenotype in *Arabidopsis* plants (van Schie et al. 2007a). These data have provided solid evidence that the level of GPPS controls the biosynthesis of GAs. Besides these in vivo data, in vitro biochemical assays have shown that GPPS is associated with the formation of different chain length of terpenes.

Our results provide indirect evidence to support one hypothesis that GPP can be transported from plastids to the cytosol. As well understood, the product of GPPS is GPP, the key precursor of monoterpenes and diterpenes synthesized in plastids and of sesquiterpenes and triterpenes in the cytosol (Fig. 1). In our study, the synthetic PTP-MpGPPS was targeted in the plastids (Fig. 2d). GC–MS-based profiling revealed that amyrin was increased by approximately 18 % of FW in transgenic flowers and approximately 33 % of FW in transgenic stems compared with those in wild-type plants, and campesterol was increased by approximately 12 % of FW in transgenic stems. Both β-amyrin and campesterol are synthesized in the cytosol through adding IPP to GPP (Fig. 1). We also analyzed monoterpenoids in leaves and stems of transgenic and wild-type plants, given that one of our goals was to increase monoterpenoids. However, monoterpenoids were hardly detected from these two tissues of *PTP-MpGPPS* transgenic plants. This result was likely associated with a low activity of monoterpenoid synthase genes in leaves of Camelina as we reported previously (Borghi and Xie 2016). Sesquiterpenoids were hardly detectable in leaves and stems of both wild-type and *PTP-MpGPPS* transgenic plants. This result suggests a low activity of the sesquiterpenoid synthase genes in these two tissues. In addition, the level of carotenoid was not apparently increased in transgenic plants. These data suggested that GPP was increased by PTP-MpGPPS catalysis in plastids, and then it was transported to the cytosol by unknown mechanisms, in which it was further used for synthesis of triterpenoid molecules. Our results supported observations from two previous researches, one of which was an overexpression of a tomato *GPPS* in vivo (van Schie et al. 2007a), and the other of which was an *AtGPPS* analysis in vitro (Hsieh et al. 2011). Results from these two studies showed the involvement of GPPS in the formation of longer terpene chains in the cytosol. In addition, a recent study on tomato revealed that GPP could be exported from plastids to the cytosol (Gutensohn et al. 2013a). In that study, the snapdragon GPPS (SSU) coupled with a cytosolic terpene synthase (TS) could catalyze the formation of both sesquiterpenes and monoterpenes. Particularly, the coupled expression of GPPS (SSU) and TS resulted in the increase of monoterpenes in the cytosol. Furthermore, the crosstalk between the cytosol and plastids has been supported by other researches. Isotope-labeled experiments showed that IPP was exchanged between the cytosol and plastids (Dudareva et al. 2005; Roberts 2007; Wang and Ohnuma 2000). Experiments of isolation of chloroplasts, envelope membrane vesicles, and proteoliposomes demonstrated efficient transportation of IPP and GPP as well as low rates of transportation of FPP and DMAPP between the cytosol and plastids (Bick and Lange 2003).

Conclusions

A synthetic novel *PTP-MpGPPS* cDNA was introduced into plastids of *C. sativa*. The ectopic expression of PTP-MpGPPS reduced isoprene emission and promoted plant growth and early flowering, increased the production of β-amyrin and campesterol in tissues. This proof-of-concept study demonstrates that a synthetic approach is applicable to reduce the loss of photo-assimilated carbon and direct metabolic flux of carbon to plant growth and storage metabolites.

Author contribution statement Dr. De-Yu Xie designed the entire project and all experiments, involved figure preparation, data discussion, manuscript preparation, GC–MS and LC–MS and isoprene emission method development, and finalized the manuscript. Dr. Jing Xi worked gene synthesis, vector construction, genetic transformation, screening of transgenic plants, GC–MS and LS–MS data analysis, figure preparation, and manuscript preparation. Dr. Lorenzo Rossi developed methods of isoprene emission experiments, was responsible for mathematic analysis of isoprene production, and involved figure preparation for isoprene measurement and manuscript preparation. Dr. Xiuli Lin involved in GC–MS and LC–MS method development and analysis of samples.

Acknowledgments We thank Phytotron at North Carolina State University for the excellent technical assistance on plant growth. We are grateful to Dr. Jyoti Dalal for critical reading of our manuscript. This work was supported by the Department of Energy (DOE) Advanced Research Projects Agency-Energy (ARPA-E) (Project #: 554667-06858).

Compliance with ethical standards

Conflict of interest The authors declare no competing financial interests.

References

Almaarri K, Alamir L, Junaid Y, Xie D-Y (2010) Volatile compounds from leaf extracts of Juniperus excelsa growing in Syria via gas chromatography mass spectrometry. Anal Methods 2:673–677

Andersson C, Engardt M (2010) European ozone in a future climate: importance of changes in dry deposition and isoprene emissions. J Geophys Res-Atmos 115:D02303

Arneth A, Schurgers G, Hickler T, Miller PA (2008) Effects of species composition, land surface cover, CO2 concentration and climate on isoprene emissions from European forests. Plant Biol 10:150–162

Arneth A, Schurgers G, Lathiere J, Duhl T, Beerling DJ, Hewitt CN, Martin M, Guenther A (2011) Global terrestrial isoprene emission models: sensitivity to variability in climate and vegetation. Atmos Chem Phys 11:8037–8052

Augustin J, Higashi Y, Feng X, Kutchan T (2015) Production of mono- and sesquiterpenes in *Camelina sativa* oilseed. Planta 242:693–708

Berhow MA, Vaughn SF, Moser BR, Belenli D, Polat U (2014) Evaluating the phytochemical potential of camelina: an emerging new crop of old world origin. Phytochemicals—biosynthesis, function and application. Recent Adv Phytochem 44:129–148

Bick JA, Lange BM (2003) Metabolic cross talk between cytosolic and plastidial pathways of isoprenoid biosynthesis: unidirectional transport of intermediates across the chloroplast envelope membrane. Arch Biochem Biophys 415:146–154

Borghi M, Xie D-Y (2016) Tissue-specific production of limonene in *Camelina sativa* with the Arabidopsis promoters of genes BANYULS and FRUITFULL. Planta 243:549–561

Burke C, Croteau R (2002a) Geranyl diphosphate synthase from *Abies grandis*: cDNA isolation, functional expression, and characterization. Arch Biochem Biophys 405:130–136

Burke C, Croteau R (2002b) Interaction with the small subunit of geranyl diphosphate synthase modifies the chain length specificity of geranylgeranyl diphosphate synthase to produce geranyl diphosphate. J Biol Chem 277:3141–3149

Burke CC, Wildung MR, Croteau R (1999) Geranyl diphosphate synthase: cloning, expression, and characterization of this prenyltransferase as a heterodimer. PNAS 96:13062–13067

Carvalho SM, Heuvelink E, Cascais R, van Kooten O (2002) Effect of day and night temperature on internode and stem length in chrysanthemum: is everything explained by DIF? Ann Bot 90:111–118

Chang TH, Hsieh FL, Ko TP, Teng KH, Liang PH, Wang AHJ (2010) Structure of a heterotetrameric geranyl pyrophosphate synthase from mint (*Mentha piperita*) reveals intersubunit regulation. Plant Cell 22:454–467

Chen QW, Fan DJ, Wang GD (2015) Heteromeric geranyl(geranyl) diphosphate synthase is involved in monoterpene biosynthesis in *Arabidopsis* flowers. Mol Plant 8:1434–1437

Choudhury SR, Riesselman AJ, Pandey S (2014) Constitutive or seed-specific overexpression of Arabidopsis G-protein gamma subunit 3 (AGG3) results in increased seed and oil production and improved stress tolerance in *Camelina sativa*. Plant Biotechnol J 12:49–59

Ciubota-Rosie C, Ruiz JR, Ramos MJ, Perez A (2013) Biodiesel from *Camelina sativa*: a comprehensive characterisation. Fuel 105:572–577

Coll-Garcia D, Mazuch J, Altmann T, Mussig C (2004) EXORDIUM regulates brassinosteroid-responsive genes. FEBS Lett 563:82–86

Curtis MD, Grossniklaus U (2003) A gateway cloning vector set for high-throughput functional analysis of genes in planta. Plant Physiol 133:462–469

Dalal J, Lopez H, Vasani NB, Hu ZH, Swift JE, Yalamanchili R, Dvora M, Lin XL, Xie DY, Qu RD, Sederoff HW (2015) A photorespiratory bypass increases plant growth and seed yield in biofuel crop *Camelina sativa*. Biotechnol Biofuels 8:175

Dudareva N, Andersson S, Orlova I, Gatto N, Reichelt M, Rhodes D, Boland W, Gershenzon J (2005) The nonmevalonate pathway supports both monoterpene and sesquiterpene formation in snapdragon flowers. Proc Natl Acad Sci USA 102:933–938

Exton DA, Smith DJ, McGenity TJ, Steinke M, Hills AJ, Suggett DJ (2010) Application of a fast Isoprene sensor (FIS) for measuring isoprene production from marine samples. Limnol Oceanogr Meth 8:185–195

Frick S, Nagel R, Schmidt A, Bodemann RR, Rahfeld P, Pauls G, Brandt W, Gershenzon J, Boland W, Burse A (2013) Metal ions control product specificity of isoprenyl diphosphate synthases in the insect terpenoid pathway. PNAS 110:4194–4199

Gilg AB, Bearfield JC, Tittiger C, Welch WH, Blomquist GJ (2005) Isolation and functional expression of an animal geranyl diphosphate synthase and its role in bark beetle pheromone biosynthesis. PNAS 102:9760–9765

Grove MD, Spencer GF, Rohwedder WK, Mandava N, Worley JF, Warthen JD, Steffens GL, Flippenanderson JL, Cook JC (1979) Brassinolide, a plant growth-promoting steroid isolated from *Brassica napus* pollen. Nature 281:216–217

Guenther A, Karl T, Harley P, Wiedinmyer C, Palmer PI, Geron C (2006) Estimates of global terrestrial isoprene emissions using MEGAN (model of emissions of gases and aerosols from nature). Atmos Chem Phys 6:3181–3210

Gutensohn M, Orlova I, Nguyen TT, Davidovich-Rikanati R, Ferruzzi MG, Sitrit Y, Lewinsohn E, Pichersky E, Dudareva N (2013a) Cytosolic monoterpene biosynthesis is supported by plastid-generated geranyl diphosphate substrate in transgenic tomato fruits. Plant J: Cell Mol Biol 75:351–363

Gutensohn M, Orlova I, Nguyen TTH, Davidovich-Rikanati R, Ferruzzi MG, Sitrit Y, Lewinsohn E, Pichersky E, Dudareva N (2013b) Cytosolic monoterpene biosynthesis is supported by plastid-generated geranyl diphosphate substrate in transgenic tomato fruits. Plant J 75:351–363

Guy SO, Wysocki DJ, Schillinger WF, Chastain TG, Karow RS, Garland-Campbell K, Burke IC (2014) Camelina: adaptation and performance of genotypes. Field Crop Res 155:224–232

Heller H (1933) Concerning *Camelina sativa* (False Flax). Angew Chem 46:441–442

Hsiao YY, Jeng MF, Tsai WC, Chuang YC, Li CY, Wu TS, Kuoh CS, Chen WH, Chen HH (2008) A novel homodimeric geranyl diphosphate synthase from the orchid *Phalaenopsis bellina* lacking a DD(X)(2-4)D motif. Plant J 55:719–733

Hsieh FL, Chang TH, Ko TP, Wang AHJ (2011) Structure and mechanism of an *Arabidopsis* medium/long-chain-length prenyl pyrophosphate synthase. Plant Physiol 155:1079–1090

Kagale S, Koh CS, Nixon J, Bollina V, Clarke WE, Tuteja R, Spillane C, Robinson SJ, Links MG, Clarke C, Higgins EE, Huebert T, Sharpe AG, Parkin IAP (2014) The emerging biofuel crop *Camelina sativa* retains a highly undifferentiated hexaploid genome structure. Nat Commun 5:3706

Källberg M, Wang H, Wang S, Peng J, Wang Z, Lu H, Xu J (2012) Template-based protein structure modeling using the RaptorX web server. Nat Protoc 7:1511–1522

Kruczynski S, Orlinski P, Biernat K (2012) Camelina oil as a biofuel for diesel engines. Przem Chem 91:111–114

Lange BM (2015) The evolution of plant secretory structures and emergence of terpenoid chemical diversity. Annu Rev Plant Biol 66:139–159

Lee JD, Lewis AC, Monks PS, Jacob M, Hamilton JF, Hopkins JR, Watson NM, Saxton JE, Ennis C, Carpenter LJ, Carslaw N, Fleming Z, Bandy BJ, Oram DE, Penkett SA, Slemr J, Norton E, Rickard AR, Whalley LK, Heard DE, Bloss WJ, Gravestock T, Smith SC, Stanton J, Pilling MJ, Jenkin ME (2006) Ozone photochemistry and elevated isoprene during the UK heatwave of August 2003. Atmos Environ 40:7598–7613

Lee DW, Kim JK, Lee S, Choi S, Kim S, Hwang I (2008) Arabidopsis nuclear-encoded plastid transit peptides contain multiple sequence subgroups with distinctive chloroplast-targeting sequence motifs. Plant Cell 20:1603–1622

Lu C, Kang J (2008) Generation of transgenic plants of a potential oilseed crop *Camelina sativa* by Agrobacterium-mediated transformation. Plant Cell Rep 27:273–278

Martin D, Piulachs MD, Cunillera N, Ferrer A, Belles X (2007) Mitochondrial targeting of farnesyl diphosphate synthase is a widespread phenomenon in eukaryotes. Biochim Biophys Acta 1773:419–426

Monson RK, Jones RT, Rosenstiel TN, Schnitzler JP (2013) Why only some plants emit isoprene. Plant Cell Environ 36:503–516

Moser BR (2012) Biodiesel from alternative oilseed feedstocks: camelina and field pennycress. Biofuels 3:193–209

Mudalkar S, Golla R, Ghatty S, Reddy AR (2014) De novo transcriptome analysis of an imminent biofuel crop, *Camelina sativa* L. using Illumina GAIIX sequencing platform and identification of SSR markers. Plant Mol Biol 84:159–171

Murashige T, Skoog F (1962) A revised medium for rapid growth and bioassays with tobacco tissue culture. Physiol Plant 15:473–497

Nagegowda DA (2010) The small subunit of geranyl diphosphate synthase: a tool to improve aroma and flavour by metabolic engineering. J Biosci 35:167–169

Nguyen HT, Silva JE, Podicheti R, Macrander J, Yang WY, Nazarenus TJ, Nam JW, Jaworski JG, Lu CF, Scheffler BE, Mockaitis K, Cahoon EB (2013) Camelina seed transcriptome: a tool for meal and oil improvement and translational research. Plant Biotechnol J 11:759–769

Nguyen HT, Park H, Koster KL, Cahoon RE, Nguyen H, Shanklin J, Clemente TE, Cahoon EB (2014) Redirection of metabolic flux for high levels of omega-7 monounsaturated fatty acid accumulation in camelina seeds. Plant Biotechnol J 12:1–13

Olszewski N, Sun TP, Gubler F (2002) Gibberellin signaling: biosynthesis, catabolism, and response pathways. Plant Cell 14(Suppl):S61–S80

Orlova I, Nagegowda DA, Kish CM, Gutensohn M, Maeda H, Varbanova M, Fridman E, Yamaguchi S, Hanada A, Kamiya Y, Krichevsky A, Citovsky V, Pichersky E, Dudareva N (2009) The small subunit of snapdragon geranyl diphosphate synthase modifies the chain length specificity of tobacco geranylgeranyl diphosphate synthase *in planta*. Plant Cell 21:4002–4017

Park J, Nguyen KT, Park E, Jeon JS, Choi G (2013) DELLA proteins and their interacting RING finger proteins repress gibberellin responses by binding to the promoters of a subset of gibberellin-responsive genes in Arabidopsis. Plant Cell 25:927–943

Park W, Feng YF, Ahn SJ (2014) Alteration of leaf shape, improved metal tolerance, and productivity of seed by overexpression of CsHMA3 in *Camelina sativa*. Biotechnol Biofuels 7:96

Peng J, Xu J (2011) RaptorX: exploiting structure information for protein alignment by statistical inference. Proteins 79:161–171

Putnam DH, Budin JT, Field LA, Breene WM (1993) Camelina: a promising low-input oilseed. In: Janick J, Simon JE (eds) New crops, exploration, research and commercialization. Wiley, New York, pp 314–322

Rai A, Smita SS, Singh AK, Shanker K, Nagegowda DA (2013) Heteromeric and homomeric geranyl diphosphate synthases from *Catharanthus roseus* and their role in monoterpene indole alkaloid biosynthesis. Mol Plant 6:1531–1549

Roberts SC (2007) Production and engineering of terpenoids in plant cell culture. Nat Chem Biol 3:387–395

Rosenstiel TN, Potosnak MJ, Griffin KL, Fall R, Monson RK (2003) Increased CO2 uncouples growth from isoprene emission in an agriforest ecosystem. Nature 421:256–259

Schillinger WF, Wysocki DJ, Chastain TG, Guy SO, Karow RS (2012) Camelina: planting date and method effects on stand establishment and seed yield. Field Crop Res 130:138–144

Schmidt A, Gershenzon J (2008) Cloning and characterization of two different types of geranyl diphosphate synthases from Norway spruce (*Picea abies*). Phytochemistry 69:49–57

Schmidt A, Wachtler B, Temp U, Krekling T, Seguin A, Gershenzon J (2010) A bifunctional geranyl and geranylgeranyl diphosphate synthase is involved in terpene oleoresin formation in *Picea abies*. Plant Physiol 152:639–655

Schnitzler JP, Lehning A, Steinbrecher R (1997) Seasonal pattern of isoprene synthase activity in *Quercus robur* leaves and its significance for modeling isoprene emission rates. Bot Acta 110:240–243

Sharkey TD (2013) Is it useful to ask why plants emit isoprene? Plant Cell Environ 36:517–520

Sharkey TD, Singsaas EL, Vanderveer PJ, Geron C (1996) Field measurements of isoprene emission from trees in response to temperature and light. Tree Physiol 16:649–654

Sharkey TD, Singsaas EL, Lerdau MT, Geron CD (1999) Weather effects on isoprene emission capacity and applications in emissions algorithms. Ecol Appl 9:1132–1137

Shonnard DR, Williams L, Kalnes TN (2010) Camelina-derived jet fuel and diesel: sustainable advanced biofuels. Environ Prog Sustain Energy 29:382–392

Singsaas EL, Sharkey TD (2000) The effects of high temperature on isoprene synthesis in oak leaves. Plant, Cell Environ 23:751–757

Sparkes IA, Runions J, Kearns A, Hawes C (2006) Rapid, transient expression of fluorescent fusion proteins in tobacco plants and generation of stably transformed plants. Nat Protoc 1:2019–2025

Springob K, Kutchan TM (2009) Introduction to the different classes of natural products. In: Osbourn AE, Lanzotti V (eds) Plant-derived natural products. Springer, New York, pp 3–50

Sun YQ, Ponnusamy S, Muppaneni T, Reddy HK, Patil PD, Li CZ, Jiang LJ, Deng SG (2014) Optimization of high-energy density biodiesel production from *Camelina sativa* oil under supercritical 1-butanol conditions. Fuel 135:522–529

Tarshis LC, Proteau PJ, Kellogg BA, Sacchettini JC, Poulter CD (1996) Regulation of product chain length by isoprenyl diphosphate synthases. PNAS 93:15018–15023

Tholl D, Lee S (2011) Elucidating the metabolism of plant terpene volatiles: alternative tools for engineering plant defenses? In: Gang DR (ed) Biological activity of phytochemicals. Springer, New York, pp 159–178

Tracy NI, Chen D, Crunkleton DW, Price GL (2009) Hydrogenated monoterpenes as diesel fuel additives. Fuel 88:2238–2240

van Schie CC, Ament K, Schmidt A, Lange T, Haring MA, Schuurink RC (2007a) Geranyl diphosphate synthase is required for biosynthesis of gibberellins. Plant J: Cell Mol Biol 52:752–762

van Schie CCN, Ament K, Schmidt A, Lange T, Haring MA, Schuurink RC (2007b) Geranyl diphosphate synthase is required for biosynthesis of gibberellins. Plant J 52:752–762

Vandermoten S, Charloteaux B, Santini S, Sen SE, Beliveau C, Vandenbol M, Francis F, Brasseur R, Cusson M, Haubruge E (2008) Characterization of a novel aphid prenyltransferase displaying dual geranyl/farnesyl diphosphate synthase activity. FEBS Lett 582:1928–1934

Vandermoten S, Haubruge E, Cusson M (2009a) New insights into short-chain prenyltransferases: structural features, evolutionary history and potential for selective inhibition. Cell Mol Life Sci 66:3685–3695

Vandermoten S, Santini S, Haubruge E, Heuze F, Francis F, Brasseur R, Cusson M, Charloteaux B (2009b) Structural features conferring dual geranyl/farnesyl diphosphate synthase activity to an aphid prenyltransferase. Insect Biochem Mol Biol 39:707–716

Wang GD, Dixon RA (2009) Heterodimeric geranyl(geranyl)diphosphate synthase from hop (*Humulus lupulus*) and the evolution of monoterpene biosynthesis. PNAS 106:9914–9919

Wang KC, Ohnuma S (2000) Isoprenyl diphosphate synthases. Biochim Biophys Acta 1529:33–48

Withers ST, Keasling JD (2007) Biosynthesis and engineering of isoprenoid small molecules. Appl Microbiol Biotechnol 73:980–990

Wu S, Schalk M, Clark A, Miles RB, Coates R, Chappell J (2006) Redirection of cytosolic or plastidic isoprenoid precursors elevates terpene production in plants. Nat Biotech 24:1441–1447

Yang T, Davies PJ, Reid JB (1996) Genetic dissection of the relative roles of auxin and gibberellin in the regulation of stem elongation in intact light-grown peas. Plant Physiol 110:1029–1034